Climate change impact over the photodegradation of PAHs in soil: characterization and metabolites identification

Montse Marquès [a,b], Montse Mari [a,b], Carme Audí-Miró [c], Jordi Sierra [b,d], Albert Soler [c], Martí Nadal [a,*], José L. Domingo [a]

[a] *Laboratory of Toxicology and Environmental Health, School of Medicine, IISPV, Universitat Rovira i Virgili, Sant Llorenç 21, 43201 Reus, Catalonia, Spain*

[b] *Environmental Engineering Laboratory, Departament d'Enginyeria Quimica, Universitat Rovira i Virgili, Av. Països Catalans 26, 43007 Tarragona, Catalonia, Spain*

[c] *Grup de Mineralogia Aplicada i Geoquímica de Fluids, Departament de Cristal·lografia, Mineralogia i Dipòsits Minerals, Facultat de Geologia, Universitat de Barcelona (UB), Martí i Franquès s/n, 08028 Barcelona, Spain.*

[d] *Laboratory of Soil Science, Faculty of Pharmacy, Universitat de Barcelona, Av. Joan XXIII s/n, 08028 Barcelona, Catalonia, Spain*

---

* Corresponding author. Tel.: +34 977 758930; fax: +34 977 759322.

E-mail address: marti.nadal@urv.cat (M. Nadal).

ABSTRACT

Keywords:
Climate change
Polycyclic aromatic hydrocarbons (PAHs)
Photodegradation
Metabolites
Hydrogen isotopes

1. Introduction

The reconstruction of past climate conditions of the Earth has demonstrated that climate has been continuously changing. However, past changes have rarely been as quick as nowadays, with human influence playing a key role [1, 2]. Human-caused greenhouse gases are driving to an increase of the global temperature, which is widely known as climate change. Climate-induced changes strongly differ throughout the globe, especially along latitudinal gradient [3]. Although the high latitude regions will suffer the greatest warming [4], the Mediterranean basin has been identified as one of the most vulnerable regions, since it lies in a transition zone between arid and temperate/rainy climates [5-9]. Moreover, the Mediterranean area has been identified as one of the world's regions where projected future increases in greenhouse gases (GHG) concentrations are most likely to cause significant changes in climate during the 21st century, with a high degree of consistency among different projections [10, 11]. The Fifth Assessment Report of the Intergovernmental Panel on Climate Change (IPCC) predicted an increase of the mean global temperature by 1 to 1.5 °C in the period 2016–2035, resulting in an increase of up to 4.8ºC at the end of the century, with respect to temperatures registered between 1850 and 1900 [12].

One of the consequences of the climate change is its potential to alter the environmental fate and transport of semi-volatile organic compounds (SVOCs) at environmentally relevant levels of human exposure [13]. Temperature has a large influence on the partitioning of environmental pollutants in the atmosphere as well as in soil and water [4, 14]. Moreover, the increase of the temperature may enhance the mobilization of organic contaminants from reservoirs such as natural waters, soils and sediments, therefore altering their rates of accumulation, sorption and degradation [15]. Therefore, because reactivity, adsorption and accumulation, are temperature-dependent processes climate change can influence every step along the transport and redistribution pathways [15-18].

Polycyclic aromatic hydrocarbons (PAHs) are a group of SVOCs composed of two or more benzene and/or pentacyclic aromatic rings [19]. PAHs may enter the environment from both natural (e.g. plant synthesis, organic matter diagenesis, and forest fires) and anthropogenic sources [20]. These include on one hand, the release of petrogenic PAHs through accidental oil spills and urban runoff [21, 22], and on the other one, pyrolytic processes, such as the incomplete combustion of organic materials during the industrial activities, residential heating, power generation, incineration and vehicle emissions [23]. Generally, anthropogenic factors have a higher impact on PAH distribution in urban areas, whereas natural factors affect their distribution in remote areas. PAHs have become a major pollutant in urban areas, as a consequence of the emissions of heavy and light traffic [24-26].

Some PAHs are resistent to biodegradation, susceptible to bioaccumulation being also identified as potential carcinogenic. Although PAHs are present in all environmental components [27], they tend to deposit via dry and wet processes on the soil top layer [28], becoming a special sink due to the PAH affinity to soil organic matter [29, 30]. Moreover, PAHs can be transformed to more toxic compounds by chemical reactions such as sulfonation, nitration, photo-oxidation, or photodegradation [23].

Compound-Specific Isotope Analysis (CSIA) is a valuable tool to control the natural degradation of pollutants in the environment, where other naturally occurring processes such as dispersion, volatilization or sorption also take place. Among these non-destructive processes, CSIA is capable to discriminate natural degradation reactions. The discrimination is based on the enrichment in heavy isotopes in the remaining substrate of a reaction due to the fact that light isotopes (e.g., ^{12}C, ^{1}H, ^{35}Cl) react faster than heavy isotopes (e.g., ^{13}C, ^{2}H, ^{37}Cl). Therefore, significant changes in isotope ratios (^{13}C/^{12}C, ^{2}H/^{1}H, ^{37}Cl/^{35}Cl) over time and/or space can be used to monitor the existence of degradation at contaminated sites [31]. Moreover, the enrichment factor –ε- value of a specific degradation process, which relates to the amount of hydrogen isotope change with the concentration variation produced due to the process of study, makes possible to calculate the fraction of compound that has been degraded through a specific degradation process.

Bergmann et al. [32] investigated hydrogen isotopic fractionation of naphthalene due to biodegradation, proving an average of 130‰ hydrogen isotopic fractionation of naphthalene when it was degraded by two different microbial cultures. Moreover, photodegradation was observed to produce hydrogen isotope fractionation in acetic acid and atrazine according to [33, 34]. These results were encouraging for studying the potential use of CSIA to confirm PAH degradation processes in the field [35]

As PAHs in soils have been proved to be highly influenced by temperature and solar radiation over time [36-39], this study was aimed at estimating the photodegradation rate of PAHs in soils affected by the climate change. To this purpose, laboratory experiments were conducted in a climate chamber considering the RCP 8.5 IPCC-based climate change scenario in the Mediterranean region. In addition, the hydrogen isotopic composition of some PAHs under study was investigated during the experiment to verify degradation processes already confirmed in our previous study. The levels of PAHs and hydrogen isotopes along the experiment were compared to those previously obtained when simulating a current Mediterranean climate [35]. Since photodegradation of PAHs have the potential to form reactive intermediates in soil matrix [40, 41], PAHs metabolites were identified in both climate scenarios.

2. Materials and methods

2.1. Photodegradation experiment

Details of the photodegradation experiment, including soil characteristics and contamination procedure, were given previously [35]. Briefly, two different soils with opposite characteristics were taken from the A horizon of remotes areas of Catalonia (NE of Spain): a) acidic and coarse-textured Arenosol soil, with granitic origin, and b) fine-textured Regosol soil, formed by sedimentary materials. A layer of 1 mm of soil was formed with ten grams of air-dried soil deployed in uncovered glass Petri dishes. Each soil sample was 10-times spiked with a solution containing 16 US EPA priority PAHs at 100 µg/mL in dichloromethane:benzene provided by Supelco® (99.0% purity, Bellefonte, PA, USA). Soil samples were incubated inside a Binder KBWF 240 climate chamber (Binder GmbH, Tuttlingen, Germany). In the current scenario, temperature and light intensity were set at 20ºC and 9.6W/m2, while in the climate change scenario temperature and daylight were 24ºC and 24W/m2, respectively. In both cases, humidity was kept at 40% in order to minimize any biotic reaction. Dark control samples covered with aluminum foil were exposed to the same environmental conditions in order to differentiate concentration decreases due to slow sorption, volatilization and other degradation processes from those related to photodegradation. Irradiated samples and dark controls of each soil were removed from the climate chamber the following days: 1, 2, 3, 4, 5, 6, 7, 14, and 28.

Photodegradation rates (%) were obtained from the following calculation:

$$L = \frac{C_N - C_I}{C_0} \text{ x } 100\% \qquad \text{(Equation 1)}$$

where L is the photodegradation rate at time t, C_0 is the original concentration of the analyte, C_N is the concentration of the analyte in non-irradiated soil sample at time t, and C_I is the concentration of the analyte in irradiated sample at time t.

The following equations were used to determine the PAH half-lives ($T_{1/2}$):

$$ln\frac{C_o}{C_t}=\text{k}\cdot\text{t} \qquad \text{(Equation 2)}$$

$$T_{1/2}=\frac{ln2}{k} \qquad \text{(Equation 3)}$$

Where k is the apparent constant reaction rate of the pseudo first order (1/day), t is time [days], Co is the initial PAH concentration in soil, and Ct= PAH concentration in soil at time t.

2.2. PAH extraction and analysis

PAHs were extracted from soil samples with 30 mL of a mixture of hexane/dichloromethane (1:1) (Scharlau Chemie S.A., Barcelona, Spain) by using an ultrasonic bath for 10 minutes, according to the US EPA method 3550. This step was repeated three times, filtering the solvent after finishing each ultrasonic extraction in order to assure good PAHs recoveries. Afterwards, samples were further concentrated with a rotatory evaporator as well as with a gentle stream of purified N_2. QC/QA procedure was carried out to verify the reported results. Thus, a mixture of six labeled hydrocarbons were used as surrogates: d_4-1,4-dichlorobenzene (99.8% purity), d_8-naphthalene (96.3% purity), d_{10}-acenaphthene (99.8% purity), d_{10}-phenanthrene (99.3% purity), d_{12}-chrysene (99.8% purity), and d_{12}-perylene (99.5% purity), being all of them provided by Supelco® (Bellefonte, PA, USA). In addition, d_{10}-fluorene (98.3% purity, Supelco®, Bellefonte, PA, USA) as well as d_{12}-benzo(*a*)pyrene (98.5% purity, Supelco®, Bellefonte, PA, USA) were used as internal standards for analytical control, being added to samples prior to analysis. A Hewlett-Packard G1099A/MSD5973 equipment with a DB-5 5% Phenyl Methyl Siloxane column (60 m x 0.25 mm x 0.25 µm) was used for quantification of the 16 PAHs under study. One µL of sample was injected at 310 ºC in pulsed splitless mode. Transfer line temperature was set at 280 ºC. The carrier gas was ultra-pure (99.9999%) helium, at a total flow rate of 1.4 mL/min. The GC oven temperature started at 90ºC, being increased at 15ºC/min until 200ºC, and at 6ºC/min up to 320ºC, and finally held at 320ºC for 20 minutes. The detector was set to quantify the analytes covering specific masses ranging from 40 to 350 atomic mass units (AMU). The mass spectrometer and source temperatures were 150ºC and 230ºC, respectively. A five-point calibration curve (20, 30, 50, 70 and 80 µg/mL) was done for PAHs quantification. Sample preparation for the concentration analyses was performed in the "Laboratory of Environmental Engineering", while GC-MS analyses was carried out at the "Servei de Recursos Científics i Tècnics" of the Universitat Rovira i Virgili (SRCiT-URV).

2.3. Metabolites identification

In order to identify PAHs metabolites, chromatograms obtained when simulating both climate scenarios [35], as well as those obtained in the present study in both soils were examined in detail by using the ChemStation library. Possible pathways of such byproducts formed in samples under light exposure for both soils and climate scenarios were further studied. Metabolites identification was also performed at the "Servei de Recursos Científics i Tècnics" of the Universitat Rovira i Virgili (SRCiT-URV).

2.4. Hydrogen isotope analysis of PAHs

For hydrogen isotope analysis of naphthalene, acenaphtene, fluorene, phenantrene, anthracene, pyrene and benzo(*a*)pyrene, PAHs were extracted from duplicate samples prepared specifically for this isotopic study. The extraction method was the same as for concentration analysis, being the extract dissolved in 62.5 µL of dichloromethane (99.5%, Scharlau Chemie S.A., Barcelona, Spain). No labeled deuterated PAHs were added to samples because they could interfere the δ^2H analysis. Since the isotope composition of a compound does not depend on its concentration, total mass recovery is not crucial for hydrogen isotopes analysis. The hydrogen isotope composition of each one of the 7 individual PAHs was analyzed using a gas chromatography-pyrolysis-isotope ratio mass spectrometry system (GC-TC-IRMS), consisting of a Trace GC Ultra equiped with a split/splitless injector, coupled to a Delta V Advantage IRMS (Thermo Scientific GmbH, Bremen, Germany) through a combustion interface. The column used in the GC/Pyr/IRMS system was an Agilent Technologies DB-1 column (30 m × 0.25 mm, 1.0 μm film thickness; Santa Clara, CA, USA). The oven temperature program started at 50°C for 1 min, was heated until 160°C at a rate of 25°C min^{-1}, then up to 320°C at a rate of 3 °C min^{-1}, being finally held at 320°C for 20 min. The injector was set to splitless mode at a temperature of 280 °C. Helium was used as a carrier gas with a gas flow rate of 1.0 mL min^{-1}.

Hydrogen isotope ratios are reported in relation to the international standard Vienna Standard Mean Ocean Water (VSMOW), using the delta notation, δ^2H (‰) = $(R/(R_{std}-1)) \times 1000$; where R and R_{std} are the isotope ratios ($^2H/^1H$) of the sample and the standard, respectively. Measurements were run in duplicate, achieving standard deviations of the duplicates of δ^2H values below ±10‰. The analytical system was daily verified using PAH control standards with known hydrogen isotope ratios, which were determined previously using a Carlo-Erba 1108 (Carlo-Erba, Milano, Italy) elemental analyzer (EA) coupled in continuous flow to a Delta Plus XP isotope ratio mass spectrometer (Thermo Fisher Scientific, Bremen, Germany). Samples preparation for the isotopic analyses were done in the "Mineralogia Aplicada i Geoquímica de Fluids" Research Group laboratory and analyzed at the "Centres Cientifics i Tecnològics" of the Universitat de Barcelona (CCiT-UB).

3. Results and discussion

3.1. Photodegradation of PAHs

The concentration changes of naphthalene, anthracene, pyrene, benzo(*a*)pyrene and benzo(*g,h,i*)perylene, as representatives of 2-, 3-, 4-, 5-, and 6- ringed PAHs, respectively, in Arenosol and Regosol soils exposed for 28 days to current (T=20ºC; light intensity=9.6 W/m^2) and climate change scenario (T= 24ºC; light intensity= 24 W/m^2), are depicted in Fig. 1 and Fig. 2. The complete list of photodegradation rates of the 16 PAHs under study on the 28th day of light exposure is summarized in Table 1. Half-lives for 16 PAHs in both soils and both simulated scenarios are shown in Fig. 3.

In agreement with previous findings [35], three main processes might be related to concentration decreases at the experimental conditions of this study: volatilization, sorption, and photodegradation. Nevertheless, the contribution of each process was different according to the physicochemical properties of each compound, the texture of each soil, and the climate conditions. In general terms, higher photodegradation rates were noted in PAHs when simulating a climate change scenario than the current climate scenario in Arenosol soil. In contrast, fewer differences in photodegradation rates were found in fine-textured Regosol soil when comparing both scenarios.

In the current scenario [35], concentrations of naphthalene were the same in irradiated and dark control samples, indicating that it was not photodegraded in any of the soils. In the climate change scenario, naphthalene was not detected in any soil sample, either irradiated or dark control, which could be due to the volatilization related to the increase of temperature. Our findings agree with Cabrerizo et al. [42], who reported a higher volatilization of low molecular weight PAHs in correlation with the temperature. Acenaphthylene also decreased dramatically its concentration under climate change conditions. However, this reduction was not as quick as that of naphthalene, achieving undetected levels after 1st and the 7th day of soil incubation in coarse- and fine- textured soil, respectively. Similarly to naphthalene, volatilization would be playing a key role in the loss of acenaphthylene. In contrast, in the current scenario both compounds could be detected at the end of the experiment in both soils [35].

In Arenosol soil, photodegradation rates of acenaphthene, fluorene, phenanthrene and anthracene in the climate change scenario (21.3%, 14.5%, 16.0% and 85.4%, respectively) were notably higher than those obtained in the current climate scenario (1.5%, 2.9%, 11.2% and 19.7%, respectively) [35]. It evidences that an increase of temperature and light enhances photodegradation. Moreover, only under more extreme conditions, acenaphthene, anthracene and fluorene were undetected in soil after 1, 4 and 14 days of light exposure, respectively. In contrast to Arenosol soil, similar photodegradation rates were found in fine-textured Regosol soil in both climate scenarios. Acenaphthene, fluorene, phenanthrene and anthracene showed photodegradation rates of 2.0%, 9.5%, 33.2% and 39.8% according to current climate scenario, while the loss of these compounds in the climate change scenario was 2.6%, 7.8%, 30.5% and 36.4%, respectively. However, anthracene was completely photodegraded in soil when increasing the temperature and light intensity after the 14 days of incubation. Our results are in agreement with those previously reported by Coover and Sims [43], who found different loss rates of 3-ringed PAHs according to the temperature (10ºC, 20ºC and 30ºC).

In Arenosol soil, fluoranthene, pyrene, benzo(*a*)anthracene + chrysene and benzo(*b*+*k*)fluoranthene were highly photodegraded under climate change conditions, showing photodegradation rates of 28.9%, 60.1%, 41.0% and 20.2%, respectively. In contrast, no photodegradation was noted for the same PAHs in the current climate scenario where soil concentrations remained constant in both irradiated and dark control samples [35]. These results agree with those of Maliszewska-Kordybach [44], who identified 4-ringed PAHs as the most sensitive to temperature change. Finally, no differences in photodegradation rates were observed in fine-textured Regosol soil, irrespective of the climate scenario. Zhang et al. [45] reported a higher photodegradation of pyrene under UV light irradiation in a fine-textured soil, with loss rates of 25% and 35% at 20ºC and 25ºC, respectively. In turn, lower rates were observed in both soils (17.1% and 18.6% in Arenosol and Regosol, respectively), probably because of differences on the light spectrum, since it is blank light exposure in our experiment.

Benzo(*a*)pyrene, benzo(*ghi*)perylene, dibenzo(*ah*)anthracene and indeno(*123-cd*)pyrene presented a similar pattern to that of 3- ringed PAHs. The increase of temperature and light intensity enhanced the photodegradation of these PAHs in Arenosol soil. Photodegradation rates of benzo(*a*)pyrene, benzo(*ghi*)perylene, dibenzo(*ah*)anthracene and indeno(*123-cd*)pyrene increased from 23.0%, 3.6%, 2.0% and 11.7%, respectively, to 54.6%, 27.1%, 37.0% and 39.1% after the increase of temperature and light related to the climate change. In fine-textured Regosol soil, these PAHs underwent more similar photodegradation rates under both simulated scenarios. Moreover, benzo(*a*)pyrene was completely lost before finishing the experiment regardless the climate conditions.

Half-lives of PAHs in soils determined on the basis of Equations 2 and 3, confirmed the results (Fig. 2). Lower half-lives were noted for the most volatile compounds (e.g., acenaphthylene and acenaphthene), due to their volatilization, as well as for those that were faster photodegraded (e.g., anthracene and benzo(*a*)pyrene). In Arenosol soil, most of PAHs presented lower half-lives when simulating the climate change scenario, while they were similar in fine-textured Regosol soil in both scenarios.

[35] Higher degradation rates of PAHs were found in fine textured Regosoil soil. Soil texture plays a key role in the photodegradation of these chemicals. Xiaozhen et al. [39] showed that the photolytic depth increases gradually from sand through silt to clay. Therefore, photochemical reactions may be accelerated when soil particles are smaller. Moreover, it has also been pointed out the important role of the photocatalysts content (manganese, magnesium, zinc, iron and aluminum oxides) in soil over PAH degradation rates [46, 47]. In contrast with Regosol soil, PAHs photodegradation rates clearly increased in Arenosol soil after applying climate change conditions. It would be related to the need of more activation energy (increase of temperature and light intensity) to achieve the photodegradation of compounds under study in Arenosol soil. ~~The higher amount of oxides in fine-textured soil than in Arenosol soil, favors PAHs photodegradation even with no increase of temperature and light intensity.~~ This fact highlights the high importance of soil properties on the PAH degradation and the difficulty of comparing our results with those from the scientific literature. High photodegradation rates reported in the present study lead to low half-lives in comparison to data from other studies. In turn, there was an agreement on the volatilization and the enhanced degradation of mid-molecular weight PAHs [43, 44, 48]. By contrast, high molecular weight PAHs are very recalcitrant in soil, even when increasing the temperature up to 30ºC [43, 44]. In current experiments benzo(*a*)pyrene was more easily photodegraded when increasing the temperature under light exposure [47]. Nonetheless, it has to be highlighted that our experiment not only considered the increase of temperature but also the light intensity, and therefore the different results with other studies might be related to this last parameter.

As it has been previously suggested by [49], there might be a synergistic effect of PAH photodegradation when both temperature and light intensity are increased. Furthermore, working with 2 environmental parameters makes more difficult the comparison between studies.

3.2. PAHs metabolites identification

PAH metabolites were identified in irradiated samples and dark controls in both soils and under both climate scenarios (Table 2). Potential pathways for the formation of these PAH metabolites are shown in Figure 4 and Figure 5.

Up to 7 metabolites were identified when simulating the current Mediterranean climate (Figure 4). Benzo(*a*)anthracene-7,12-dione was identified only under light condition, while, 9,10-anthracenedione was formed under light and dark conditions. The oxidation of anthracene and benzo(*a*)anthracene may lead to the formation of 9,10-anthracenedione and benzo(*a*)anthracene-7,12-dione, respectively, as a consequence of photodegradation or other degradation processes [41, 50, 51]. 9,10-anthracenedione was found after 2 and 3 days of light exposure in fine-textured Regosol and Arenosol soils, respectively. It was also found in dark controls after 14 days of soil incubation proving that unknown degradation processes could be also occurring in the dark. In addition, light could also enhance the oxidation of anthracene, driving to a faster formation of 9,10-anthracenedione. Although benzo(*a*)anthracene was only photodegraded in fine-textured Regosol soil, benzo(*a*)anthracene-7,12-dione was identified in fine-textured Regosol soil as well as Arenosol soil after 14 and 28 days of light exposure, respectively. It points out that a slight degradation takes place in Arenosol soil. These same metabolites which were found in the current climate scenario were also identified under climate change conditions (Figure 5). 9,10-anthracenedione was found just the first day of incubation in both soils, in either irradiated samples and dark controls. Benzo(*a*)anthracene-7,12-dione was identified after 2 and 3 days of light exposure in fine-textured Regosol and Arenosol soils, respectively. Hence, the formation of 9,10-anthracenedione as well as of benzo(*a*)anthracene-7,12-dione depends on soil texture and climate conditions. In contrast to concentration data, the increase of temperature and light intensity enhanced byproducts formation in Regosol soil. Concentration data must be combined with metabolites. In consequence, PAH levels in soil can be influenced by volatilization and/or sorption/desorption processes, while metabolites clearly give evidence of degradation.

The increase of the temperature as well as the light intensity lead to the formation of new metabolites under climate change conditions (Figure 5). Acenaphthylene and benzo(*a*)anthracene-7,12-dione could have been transformed into naphthalic anhydride [50], which was detected after 3 and 5 days of light exposure in fine-textured Regosol and Arenosol soils, respectively. However, it was not detected between the 3rd and the 6th day in fine-textured Regosol soil, being the most plausible hypothesis dynamics -degradation and creation- of such metabolite. Furthermore, there were some byproducts that were formed depending on the soil. In Arenosol soil, acenaphthylene and fluorene, which were completely lost before finishing the experiment, may be oxidized and transformed into oxy-PAHs. Woo et al. [41] reported that the photodegradation of acenaphthylene leads to the formation of 1(2H)-acenphthylenone. On the other hand, Acevedo et al. [52] reported that fluorene leads to the formation of 9H-fluorene-9-one when studying PAHs biodegradation. However, since negligible oxygen consumption was reported in this experiment [35], any biodegradation process may be disregarded. Hence, the occurrence of such metabolite on the 6th day of light exposure might come from the oxidation of fluorene, finding the key role on the light exposure.

Since the 1st day, light exposure might have hydroxilized acenaphthene by attaching an -OH radical, ultimately generating acenaphthenol [41] since the 1st day. Furthermore, naphthalene oxidation might create 2-naphthalenecarboxaldehyde after 5 days in fine-textured soil, therefore discarding volatilization as the only process occurring in Regosol soil. However, our findings need further confirmation.

The intermediate chemicals identified in the present study were quinones, ketones and aldehydes, whose high stability allows a higher resistance to degradation. However, although undetected, it cannot be discarded that intermediate compounds with lower stability may be formed, but quickly degraded. Moreover, the experiment was focused on the assessment of the 16 US EPA priority PAHs, and the identification and description of PAHs metabolites might be somehow biased.

3.3 Hydrogen isotopes of PAHs

In a context of climate change, benzo(*a*)pyrene showed a significant hydrogen isotope fractionation over time in both Arenosol and Regosol soils (Figure 6). Additionally, a significant enrichment in ^{2}H in benzo(*a*)pyrene was also observed in dark controls from both types of soil.

In Arenosol soil, benzo(*a*)pyrene of irradiated samples experienced hydrogen isotopic fractionation with a change in benzo(*a*)pyrene hydrogen isotopic composition from -6‰ to +29‰ after 5 days of experiment. In Regosol soil, a similar variation in hydrogen isotopic composition of benzo(*a*)pyrene was obtained (from -6‰ to +55‰ after 3 days of experiment). These results are in agreement with the concentration results, confirming the degradation of benzo(*a*)pyrene under climate change conditions. Hydrogen isotopic changes of benzo(*a*)pyrene in dark controls (from -6‰ to +115‰ after 7 days of incubation in Arenosol soil, and from -6‰ to +129 ‰ after 4 days of incubation in Regosol soil) confirm its degradation in the dark, being in agreement with the formation of metabolites under these conditions. Although none of the metabolites was linked to benzo(*a*)pyrene, non-stable byproducts could have been generated but quickly degraded. Therefore, the presence of unknown degradation processes of PAHs occurring also in the dark was confirmed from two lines of evidence: 1) metabolites formation from other PAHs, and 2) hydrogen isotopic fractionation of benzo(*a*)pyrene (Figure 6).

When comparing the hydrogen isotope fractionation of benzo(*a*)pyrene under both climate scenarios, a very similar trend was observed. However, a much higher degree of hydrogen isotope fractionation was achieved under current climate conditions in both Arenosol and Regosol soil. In Arenosol soil, under current climate conditions a total hydrogen isotopic change of 232 ‰ was obtained after 5 days in irradiated samples while a 35‰ hydrogen isotopic fractionation was found under climate change conditions after the same period of time. In Regosol soil, a 107‰ hydrogen isotope fractionation of benzo(*a*)pyrene was obtained in the current climate conditions after 3 days of incubation [35], being higher than (indicar valor, no?) that in soils affected by climate change. These results indicate a less hydrogen isotope discrimination under climate change. In contrast, climate change might lead a higher hydrogen isotope fractionation in the darkness in both soils. In Arenosol soil a total fractionation of 121‰ was achieved after 7 days in a climate change context, while after the same period of time a fractionation of 81‰ was achieved when soils were exposed to current climate conditions [35]. Finally, in Regosol soil, the fractionation was 136‰ vs. 74‰ in the climate change and current scenarios, respectively.

The differences in the degree of hydrogen isotope fractionation observed between the different climate conditions, including darkness conditions, as well as with different types of soil, suggest that hydrogen isotope fractionation could discriminate different types of degradation. However, the presence of other processes occurring along the experiment such as volatilization and sorption, made impossible the calculation of the Ɛ value.

In order to obtain the Ɛ value specific of each degradation process, future studies should try to avoid other processes that affect concentration variation. By comparing Ɛ values, it can be studied whether the effect on the compounds produced under the different conditions is isotopically distinguishable. Therefore, applying the Ɛ in the field, the amount of compound degraded due to the specific process should be able to be calculated.

Regarding the other six PAHs analyzed during the isotopic study (namely, naphthalene, acenaphtene, fluorene, phenantrene, anthracene and pyrene), naphthalene and acenaphtene were not detected, so no isotopic effects could be studied on them. Fluorene could not be followed neither due to interference with the deuterated fluorene used as internal standard for analytical control. Finally, phenantrene, anthracene and pyrene did not show any hydrogen isotope fractionation. According to the basis of isotopic fractionation (), the non-observation of isotopic effects on the latter three compounds could be associated to low isotopes discrimination during the bond breakage produced by photodegradation. Further studies should be made to confirm this hypothesis.

4. Conclusions

Climate change is able to impact on the photodegradation of PAHs depending on the exposure time, the molecular weight of each compound, and the soil texture. According to our findings, when increasing the temperature and light intensity, low molecular weight PAHs are faster volatilized. Moreover, medium and high molecular weight PAHs presented higher photodegradation rates in Arenosol soil, while their rates remained constant in fine-textured Regosol soil, irrespective of the climate scenario. The important role of the required activation energy was confirmed as it favours the photodegradation reactions in different soils. The content of photocatalysts in Arenosol soil needs more temperature and light intensity to enhance the photodegradation of PAHs. In turn, photocatalysts in fine-textured Regosol soil are capable to faster the photodegradation of PAHs under any climate condition. Moreover, it was noticed that the formation PAHs metabolites as a consequence of light exposure takes place through different pathways, being the oxidation of parent compounds the most relevant. In the climate change scenario, the formation of byproducts was clearly favoured in comparison with current climate conditions where the amount of detected metabolites was significantly lower. In consequence, in the future humans might be exposed to lower environmental concentrations but to new PAHs metabolites, which may be even more toxic [23].

Finally, hydrogen isotope results confirm that benzo(*a*)pyrene is degraded in a climate change scenario, in both light and darkness. The differences in the degree of hydrogen isotopic fractionation according to the different climate conditions and types of soil, suggest the use of hydrogen isotopes to distinguish different types of degradation. Moreover, the significant hydrogen isotopic change obtained in the different study cases represents a great potential of CSIA to be used as a powerful tool to monitor PAH degradation in the field. Furthermore, the degradation of benzo(*a*)pyrene without light intervention should be more studied in future work, since it could be a potentially relevant pathway of PAH loss in soil.

5. Acknowledgements

This study was financially supported by the Spanish Ministry of Economy and Competitiveness, through the projects CTM2012-33079, CGL2011-29975-C04-01 and CGL2014-57215-C4-1-R, and by the Catalan Government, through the projects 2014SGR90 and 2014SGR1456. Montse Marquès received a PhD fellowship from AGAUR (Commissioner for Universities and Research of the Department of Innovation, Universities and Enterprise of the "Generalitat de Catalunya" and the European Social Fund).

6. References

[1] U. Cubasch, D. Wuebbles, D. Chen, M.C. Facchini, D. Frame, N. Mahowald, J.-G. Winther, Introduction, in: T.F. Stocker, D. Qin, G.-K. Plattner, M. Tignor, S.K. Allen, J. Boschung, A. Nauels, Y. Xia, V. Bex, P.M. Midgley (Eds.) Climate Change 2013: The Physical Science Basis. Contribution of Working Group I to the Fifth Assessment Report of the Intergovernmental Panel on Climate Change, Cambridge University Press, Cambridge, United Kingdom and New York, NY, USA, 2013, pp. 119–158.

[2] L. Lamon, M.D. Valle, A. Critto, A. Marcomini, Introducing an integrated climate change perspective in POPs modelling, monitoring and regulation, Environ. Pollut. 157 (2009) 1971-1980.

[3] C.J.M. Philippart, R. Anadón, R. Danovaro, J.W. Dippner, K.F. Drinkwater, S.J. Hawkins, T. Oguz, G. O'Sullivan, P.C. Reid, Impacts of climate change on European marine ecosystems: Observations, expectations and indicators, J. Exp. Mar. Biol. Ecol. 400 (2011) 52-69.

[4] P.D. Noyes, M.K. McElwee, H.D. Miller, B.W. Clark, L.A. Van Tiem, K.C. Walcott, K.N. Erwin, E.D. Levin, The toxicology of climate change: Environmental contaminants in a warming world, Environ. Int. 35 (2009) 971-986.

[5] R.F. Bangash, A. Passuello, M. Hammond, M. Schuhmacher, Water allocation assessment in low flow river under data scarce conditions: A study of hydrological simulation in Mediterranean basin, Sci. Total Environ. 440 (2012) 60-71.

[6] M. Marquès, R.F. Bangash, V. Kumar, R. Sharp, M. Schuhmacher, The impact of climate change on water provision under a low flow regime: A case study of the ecosystems services in the Francoli river basin, J. Hazard. Mater. 263, Part 1 (2013) 224-232.

[7] M. Sánchez-Canales, A. López Benito, A. Passuello, M. Terrado, G. Ziv, V. Acuña, M. Schuhmacher, F.J. Elorza, Sensitivity analysis of ecosystem service valuation in a Mediterranean watershed, Sci. Total Environ. 440 (2012) 140-153.

[8] D. Schröter, W. Cramer, R. Leemans, I.C. Prentice, M.B. Araújo, N.W. Arnell, A. Bondeau, H. Bugmann, T.R. Carter, C.A. Gracia, A.C. De La Vega-Leinert, M. Erhard, F. Ewert, M. Glendining, J.I. House, S. Kankaanpää, R.J.T. Klein, S. Lavorel, M. Lindner, M.J. Metzger, J. Meyer, T.D. Mitchell, I. Reginster, M. Rounsevell, S. Sabaté, S. Sitch, B. Smith, J. Smith, P. Smith, M.T. Sykes, K. Thonicke, W. Thuiller, G. Tuck, S. Zaehle, B. Zierl, Ecology: Ecosystem service supply and vulnerability to global change in Europe, Science 310 (2005) 1333-1337.

[9] M. Terrado, V. Acuña, D. Ennaanay, H. Tallis, S. Sabater, Impact of climate extremes on hydrological ecosystem services in a heavily humanized Mediterranean basin, Ecol. Indic. 37, Part A (2014) 199-209.

[10] A. Mariotti, Y. Pan, N. Zeng, A. Alessandri, Long-term climate change in the Mediterranean region in the midst of decadal variability, Clim. Dyn. 44 (2015) 1437–1456.

[11] F. Giorgi, Climate change hot-spots, Geophys. Res. Lett. 33 (2006) L08707.

[12] IPCC, Climate Change 2013: The Physical Science Basis. Contribution of Working Group I to the Fifth Assessment Report of the Intergovernmental Panel on Climate Change, Cambridge University Press, Cambridge, United Kingdom and New York, NY, USA, 2013.

[13] J.M. Armitage, C.L. Quinn, F. Wania, Global climate change and contaminants-an overview of opportunities and priorities for modelling the potential implications for long-term human exposure to organic compounds in the Arctic, J. Environ. Monit. 13 (2011) 1532-1546.

[14] A. Manciocco, G. Calamandrei, E. Alleva, Global warming and environmental contaminants in aquatic organisms: The need of the etho-toxicology approach, Chemosphere 100 (2014) 1-7.

[15] R.W. Macdonald, D. Mackay, Y.-F. Li, B. Hickie, How Will Global Climate Change Affect Risks from Long-Range Transport of Persistent Organic Pollutants?, Hum. Ecol. Risk Assess. 9 (2003) 643-660.

[16] D. Schiedek, B. Sundelin, J.W. Readman, R.W. Macdonald, Interactions between climate change and contaminants, Mar. Pollut. Bull. 54 (2007) 1845-1856.

[17] UNEP, Climate Change and POPs; Predicting the Impacts, in: Report of the UNEP/AMAP expert group, United Nations Environmental Programme, 2010, pp. 65.

[18] R. Kallenborn, C. Halsall, M. Dellong, P. Carlsson, The influence of climate change on the global distribution and fate processes of anthropogenic persistent organic pollutants, J. Environ. Monit. 14 (2012) 2854-2869.

[19] L. Muckian, R. Grant, E. Doyle, N. Clipson, Bacterial community structure in soils contaminated by polycyclic aromatic hydrocarbons, Chemosphere 68 (2007) 1535–1541.

[20] M. Nadal, M. Mari, M. Schuhmacher, J.L. Domingo, Multi-compartmental environmental surveillance of a petrochemical area: Levels of micropollutants, Environ. Int. 35 (2009) 227-235.

[21] A.C. Ruiz-Fernández, J.F. Ontiveros-Cuadras, J.L. Sericano, J.-A. Sanchez-Cabeza, L.L.W. Kwong, R.B. Dunbar, D.A. Mucciarone, L.H. Pérez-Bernal, F. Páez-Osuna, Long-range atmospheric transport of persistent organic pollutants to remote lacustrine environments, Sci. Total Environ. 493 (2014) 505-520.

[22] M.B. Yunker, R.W. Macdonald, R. Vingarzan, R.H. Mitchell, D. Goyette, S. Sylvestre, PAHs in the Fraser River basin: a critical appraisal of PAH ratios as indicators of PAH source and composition, Org. Geochem. 33 (2002) 489-515.

[23] M.R. Ras, R.M. Marcé, A. Cuadras, M. Mari, M. Nadal, F. Borrull, Atmospheric levels of polycyclic aromatic hydrocarbons in gas and particulate phases from Tarragona Region (NE Spain), Int. J. Environ. Anal. Chem. 89 (2009) 543-556.

[24] Y.-F. Jiang, X.-T. Wang, F. Wang, Y. Jia, M.-H. Wu, G.-Y. Sheng, J.-M. Fu, Levels, composition profiles and sources of polycyclic aromatic hydrocarbons in urban soil of Shanghai, China, Chemosphere 75 (2009) 1112–1118.

[25] C. Wang, S. Wu, S. Zhou, H. Wang, B. Li, H. Chen, Y. Yu, Y. Shi, Polycyclic aromatic hydrocarbons in soils from urban to rural areas in Nanjing: Concentration, source, spatial distribution, and potential human health risk, Sci. Total Environ. 527-528 (2015) 375-383.

[26] M. Nadal, M. Schuhmacher, J.L. Domingo, Long-term environmental monitoring of persistent organic pollutants and metals in a chemical/petrochemical area: Human health risks, Environ. Pollut. 159 (2011) 1769-1777.

[27] A. Melnyk, A. Dettlaff, K. Kuklińska, J. Namieśnik, L. Wolska, Concentration and sources of polycyclic aromatic hydrocarbons (PAHs) and polychlorinated biphenyls (PCBs) in surface soil near a municipal solid waste (MSW) landfill, Sci. Total Environ. 530-531 18-27.

[28] M. Nadal, M. Schuhmacher, J.L. Domingo, Levels of PAHs in soil and vegetation samples from Tarragona County, Spain, Environ. Pollut. 132 (2004) 1-11.

[29] A.J. Sweetman, M.D. Valle, K. Prevedouros, K.C. Jones, The role of soil organic carbon in the global cycling of persistent organic pollutants (POPs): interpreting and modelling field data, Chemosphere 60 (2005) 959-972.

[30] B. Aichner, B.M. Bussian, P. Lehnik-Habrink, S. Hein, Regionalized concentrations and fingerprints of polycyclic aromatic hydrocarbons (PAHs) in German forest soils, Environ. Pollut. 203 (2015) 31-39.

[31] R.U. Meckenstock, B. Morasch, C. Griebler, H. Richnow, Stable isotope fractionation analysis as a tool to monitor biodegradation in contaminated acquifers, J. Contam. Hydrol. 75 (2004) 215-255.

[32] F.D. Bergmann, N.M.F.H. Abu Laban, A.H. Meyer, M. Elsner, R.U. Meckenstock, Dual (C, H) isotope fractionation in anaerobic low molecular weight (Poly)aromatic hydrocarbon (PAH) degradation: potential for field studies and mechanistic implications, Environ. Sci. Technol. 45 (2011) 6947-6953.

[33] A. Hartenbach, T. Hofstetter, T. Tentscher, S. Canonica, M. Berg, A. Schwarzenbach, Hydrogen, and nitrogen isotope fractionation during light-induced transformations of atrazine, Environ. Sci. Technol. 42 (2008) 7751–7756.

[34] Y. Oba, H. Naraoka, Carbon and hydrogen isotope fractionation of acetic acid during degradation by ultraviolet light, Geochem. J. 41 (2007) 103-110.

[35] M. Marquès, M. Mari, J. Sierra, M. Schuhmacher, J.L. Domingo, M. Nadal, Climate change effects on PAH photodegradation in Mediterranean soils: a pilot study, Organohalogen Compd. 76 (2014) 380-383.

[36] M.E. Balmer, K.-U. Goss, R.P. Schwarzenback, Photolytic transformation of organic pollutants on soil surfacess an experimental approach, Environ. Sci. Technol. 34 (2000) 1240-1245.

[37] M.P. Frank, P. Graebing, J.S. Chib, Effect of soil moisture and sample depth on pesticide photolysis, J. Agric. Food Chem. 50 (2002) 2607-2614.

[38] A. Gong, C. Ye, X. Wang, Z. Lei, J. Liu, Dynamics and mechanism of ultraviolet photolysis of atrazine on soil surface, Pest Manage. Sci. 57 (2001) 380-385.

[39] F. Xiaozhen, L. Boa, G. Aijun, Dynamics of solar light photodegradation behavior of atrazine on soil surface, J. Hazard. Mater. B117 (2005) 75-79.

[40] H. Gupta, B. Gupta, Photocatalytic degradation of polycyclic aromatic hydrocarbon benzo[a]pyrene by iron oxides and identification of degradation products, Chemosphere (2015).

[41] O.T. Woo, W.K. Chung, K.H. Wong, A.T. Chow, P.K. Wong, Photocatalytic oxidation of polycyclic aromatic hydrocarbons: Intermediates identification and toxicity testing, J. Hazard. Mater. 168 (2009) 1192-1199.

[42] A. Cabrerizo, C. Galbán-Malagón, S.D. Vento, J. Dachs, Sources and fate of polycyclic aromatic hydrocarbons in the Antarctic and Southern Ocean atmosphere, Global Biogeochem. Cycles 28 (2015) 1424-1436.

[43] M.P. Coover, R.C. Sims, The effect of temperature on polycyclic aromatic hydrocarbon persistence in an unacclimated agricultural soil, Biol. Eng. Fac. Publ. (1987) Paper 57.

[44] B. Maliszewska-Kordybach, The effect of temperature on the rate of dissapperance of polycyclic aromatic hydrocarbons from soils, Environ. Pollut. 79 (1993) 15-20.

[45] L. Zhang, C. Xua, Z. Chena, X. Li, P. Li, Photodegradation of pyrene on soil surfaces under UV light irradiation, J. Hazard. Mater. 173 (2010) 168-172.

[46] X. Zhao, X. Quan, Y. Zhao, H. Zhao, S. Chen, J. Chen, Photocatalytic remediation of γ-HCH contaminated soil induced by α-Fe_2O_3 and TiO_2, J. Environ. Sci. 16 (2004) 938-941.
[47] L. Zhang, P. Li, Z. Gong, A. Oni, Photochemical behavior of benzo[a]pyrene on soil surfaces under UV light irradiation, J. Environ. Sci. 18 (2006) 1226-1232.
[48] P. Oleszczuk, S. Baran, Degradation of individual polycyclic aromatic hydrocarbons (PAHs) in soil polluted with aircraft fuel, Pol. J. Environ. Stud. 12 (2003) 431-437.
[49] M. Nadal, J.J. Wargent, K.C. Jones, N.D. Paul, M. Schuhmacher, J.L. Domingo, Influence of UV-B radiation and temperature on photodegradation of PAHs: Preliminary results, J. Atmos. Chem. 55 (2006) 241-252.
[50] T. Cajthaml, P. Erbanová, V. Sasek, M. Moeder, Breakdown products on metabolic pathway of degradation of benz[a]anthracene by a ligninolytic fungus, Chemosphere 64 (2006) 560-564.
[51] J. Gabriel, P. Baldrian, P. Verma, T. Cajthaml, V. Merhautová, I. Eichlerová, I. Stoytchev, T. Trnka, P. Stopka, F. Nerud, Degradation of BTEX and PAHs by Co(II) and Cu(II)-based radical-generating systems, Appl. Catal. B Environ. 51 (2004) 159-164.
[52] F. Acevedo, L. Pizzul, M.d.P. Castillo, R. Cuevas, M.C. Diez, Degradation of polycyclic aromatic hydrocarbons by the Chilean white-rot fungus Anthracophyllum discolor, J. Hazard. Mater. 185 (2011) 212-219.

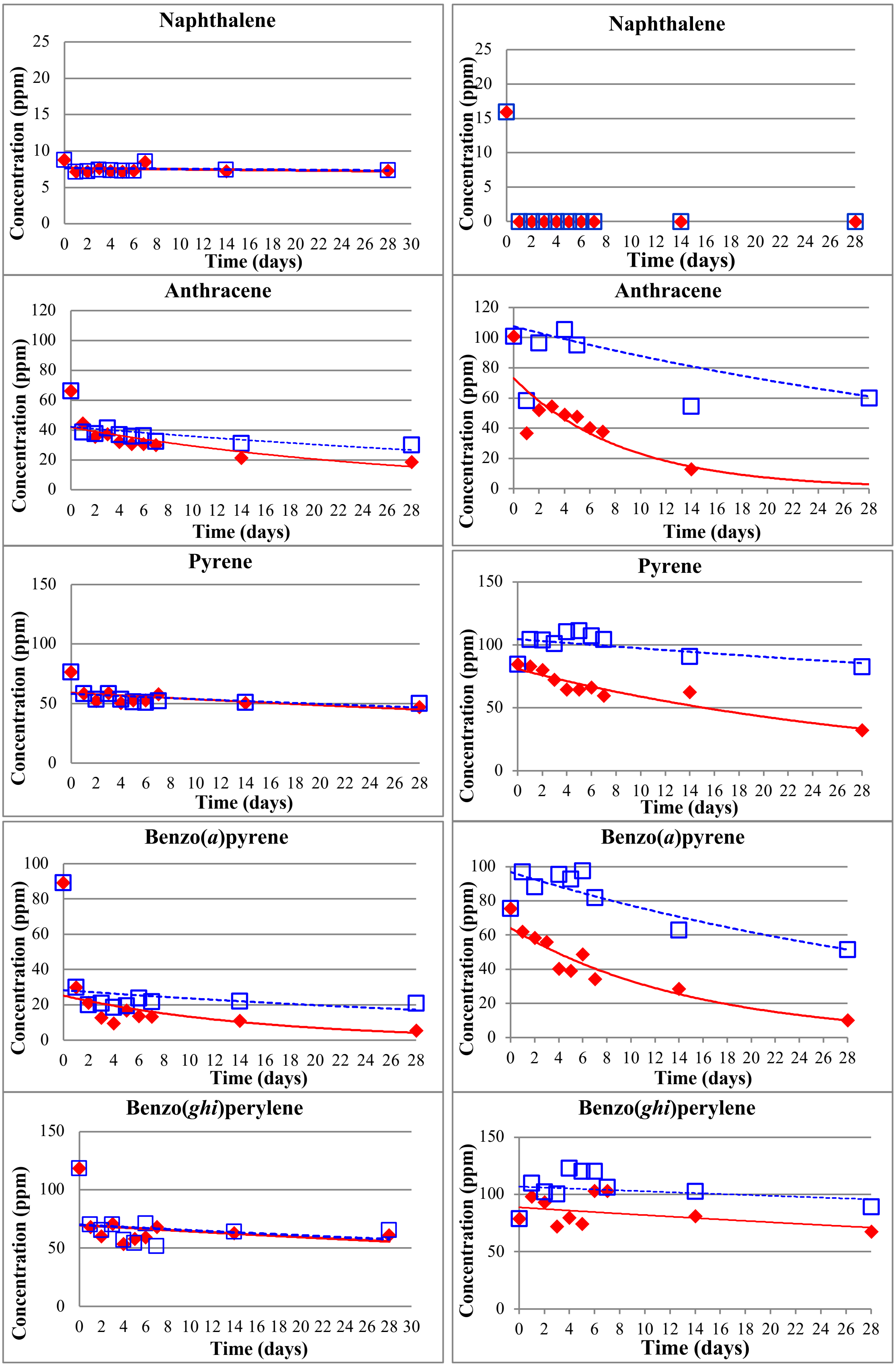

Figure 1. Concentration trends of some representatives of 2-, 3-, 4-, 5-, and 6- ringed PAHs exposed to current climate (left) and climate change (right) scenario in Arenosol soil. RSD (naphthalene)= 0.36-2.38%; RSD (anthracene)= 0.48-2.43%; RSD (pyrene)= 0.43-4.55%; RSD (benzo(*a*)pyrene)= 0.04-0.70%; RSD (benzo(ghi)perylene)= 0.01-2.64%.

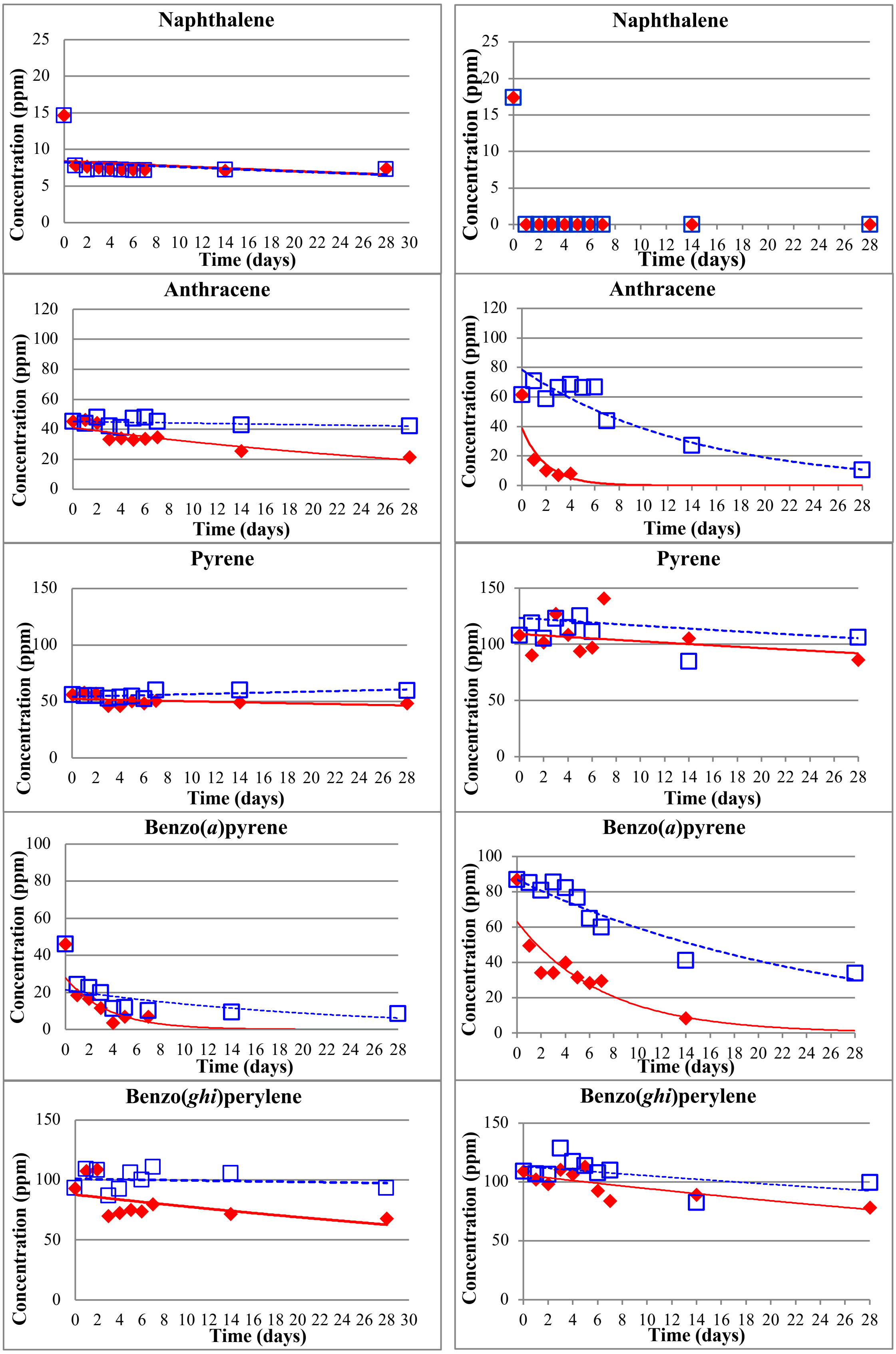

Figure 2. Concentration trends of some representatives of 2-, 3-, 4-, 5-, and 6- ringed PAHs exposed

current scenario (left) and climate change (right) scenario in fine-textured Regosol soil. RSD (naphthalene)= 0.36-2.38%; RSD (anthracene)= 0.48-2.43%; RSD (pyrene)= 0.43-4.55%; RSD (benzo(*a*)pyrene)= 0.04-0.70%; RSD (benzo(ghi)perylene)= 0.01-2.64%.

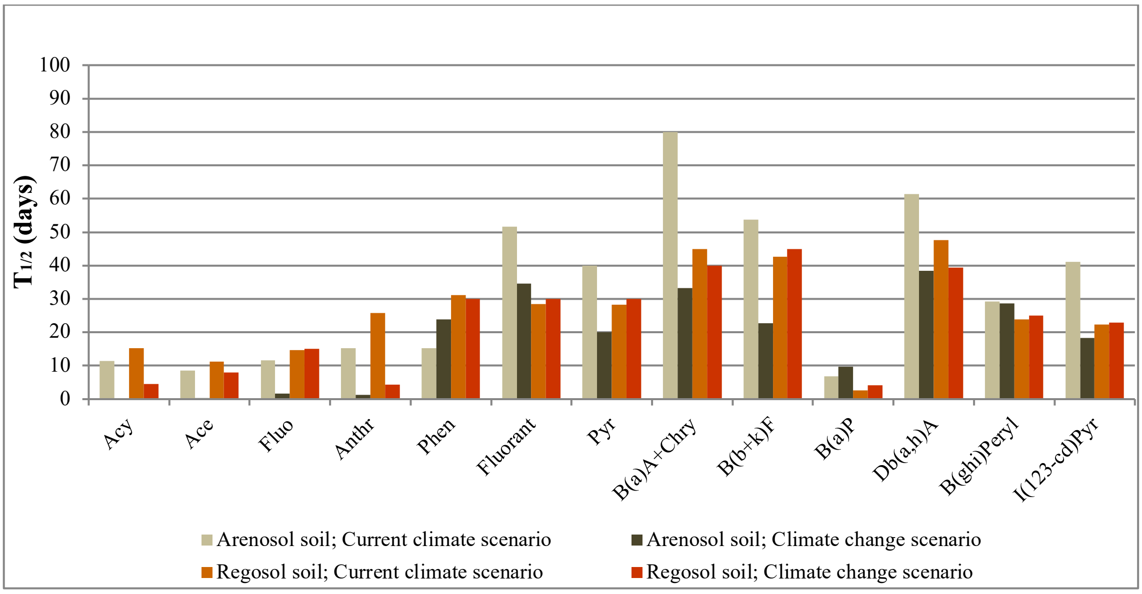

Figure 3. Half-lives of 16 PAHs exposed to the current Mediterranean climate scenario and the climate change scenario in Arenosol and fine-textured Regosol soil.

a) Arenosol soil

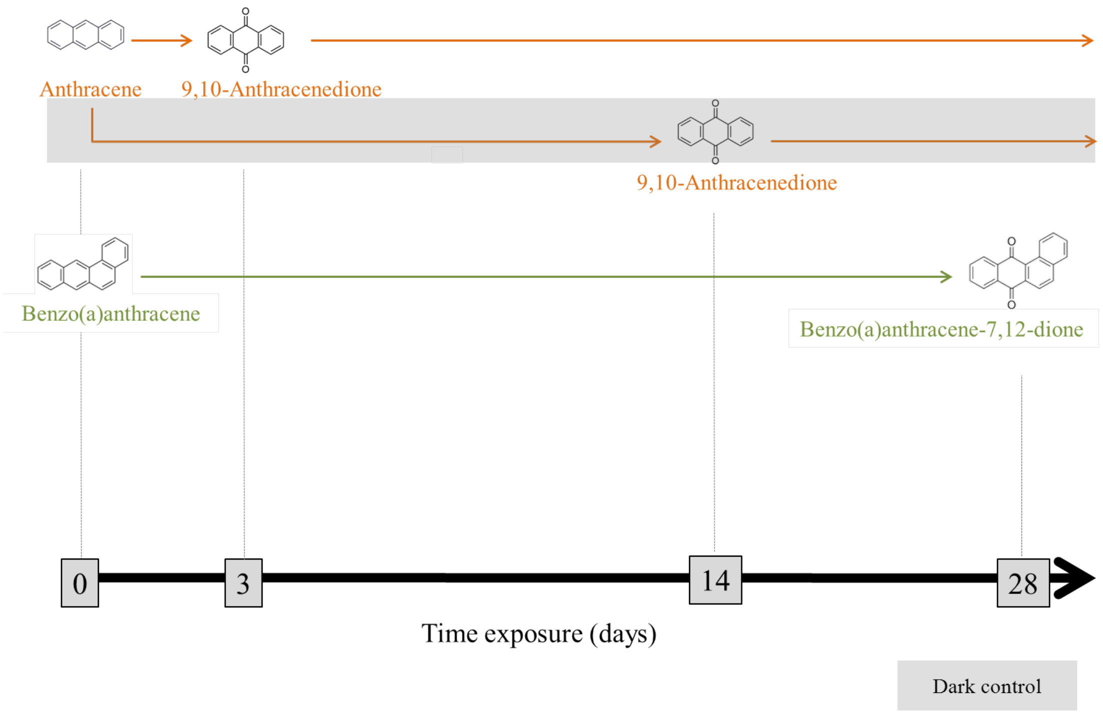

b) Fine-textured Regosol soil

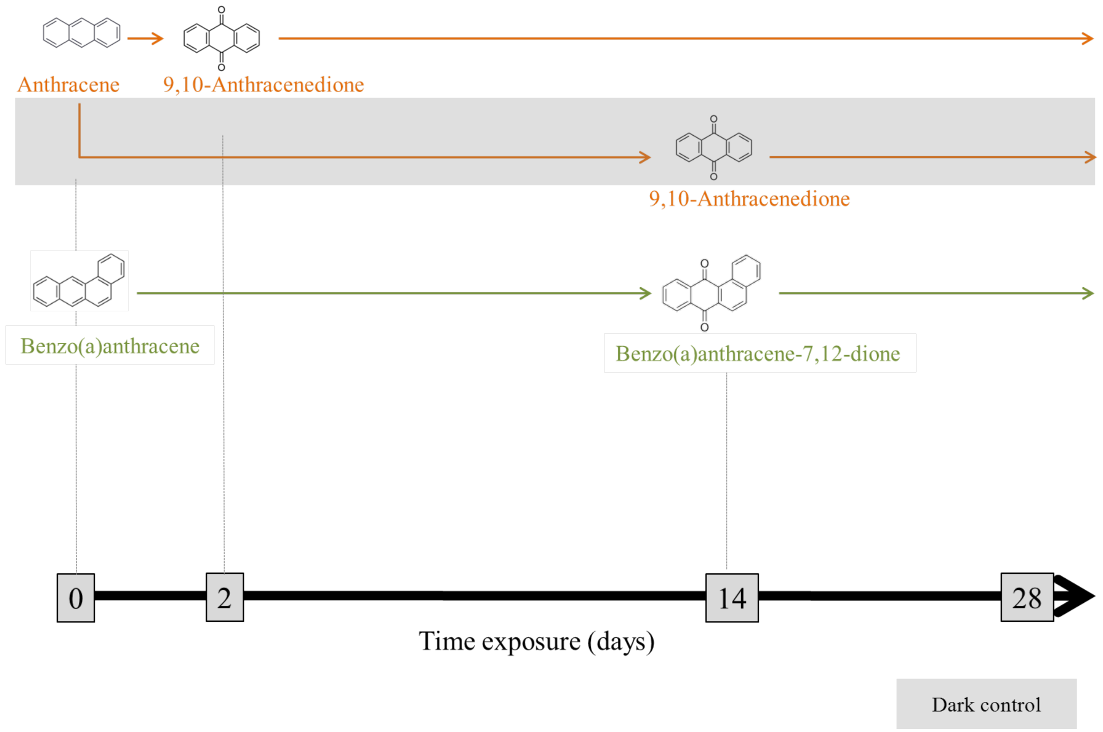

Figure 4. Photodegradation products of PAHs in a) Arenosol soil and b) fine-textured Regosol soil when simulating the current Mediterranean climate

a) Arenosol soil

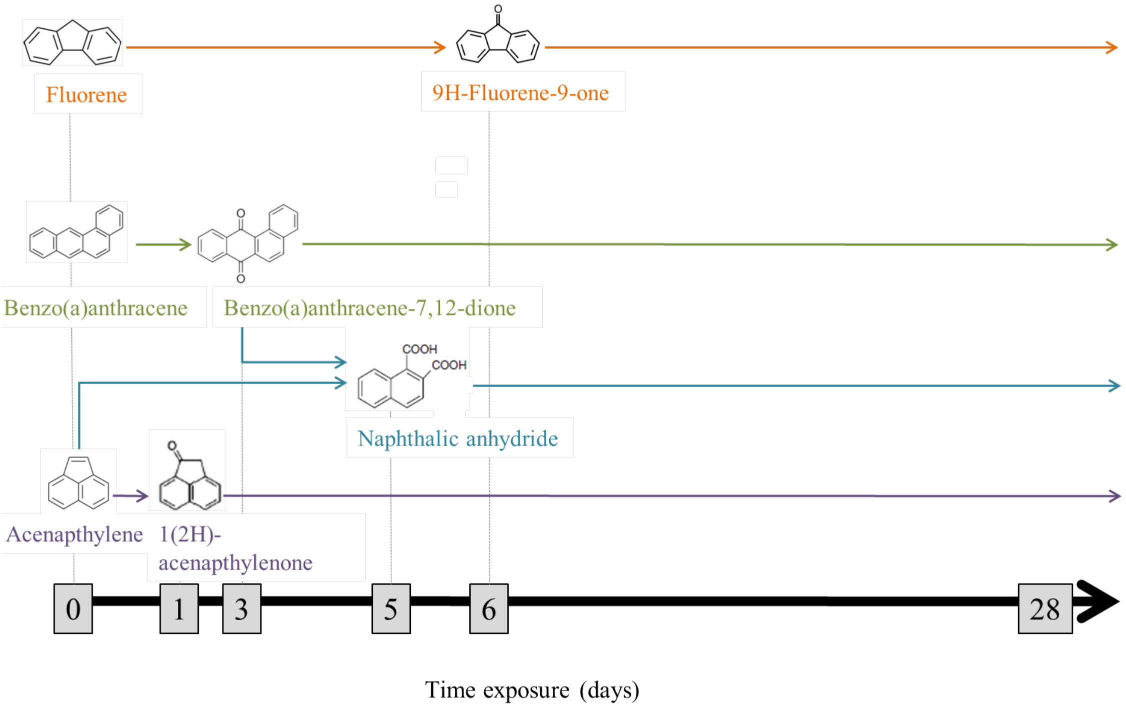

b) Fine-textured Regosol soil

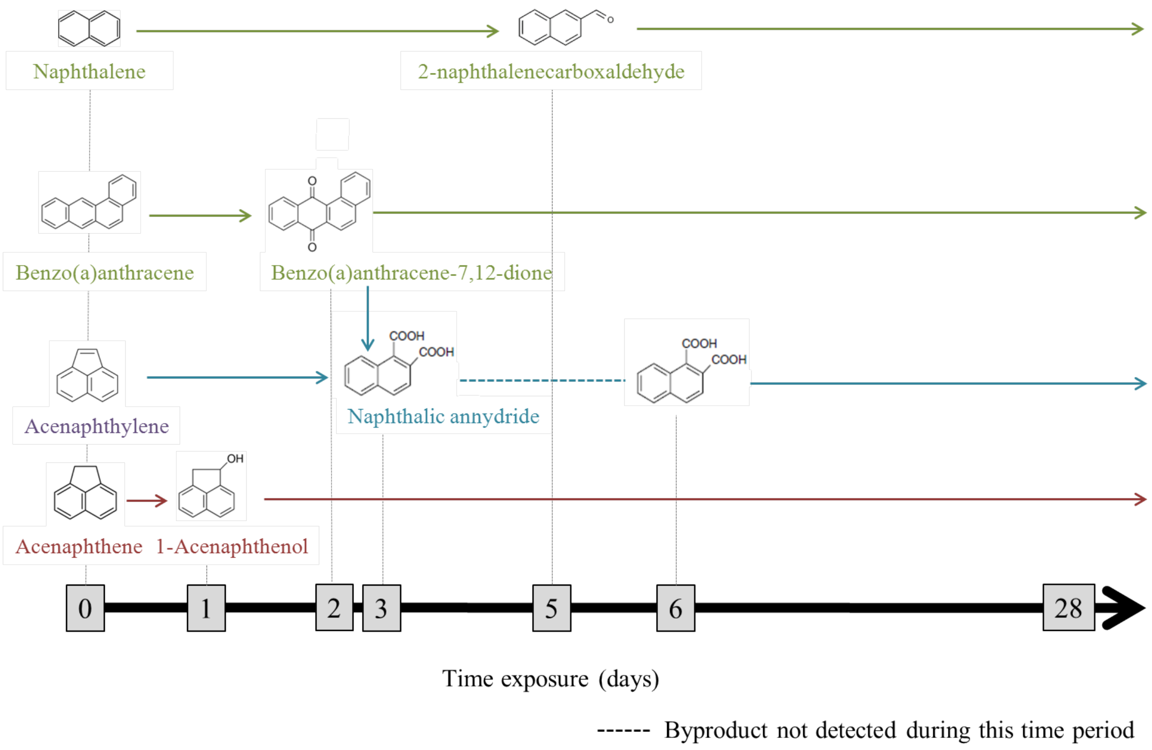

Figure 5. Photodegradation products of PAHs in a) Arenosol soil and b) fine-textured Regosol soil when simulating the IPCC-based climate change scenario in the Mediterranean region

a) Arenosol soil

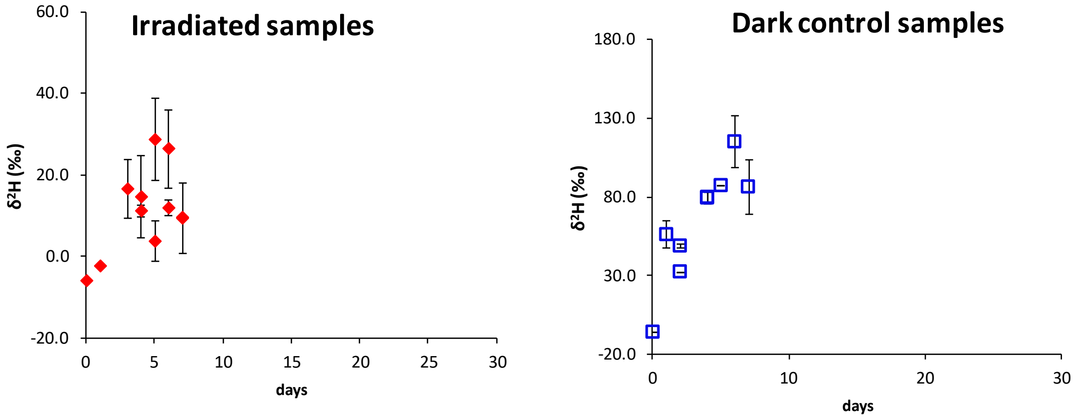

b) Fine-textured Regosol soil

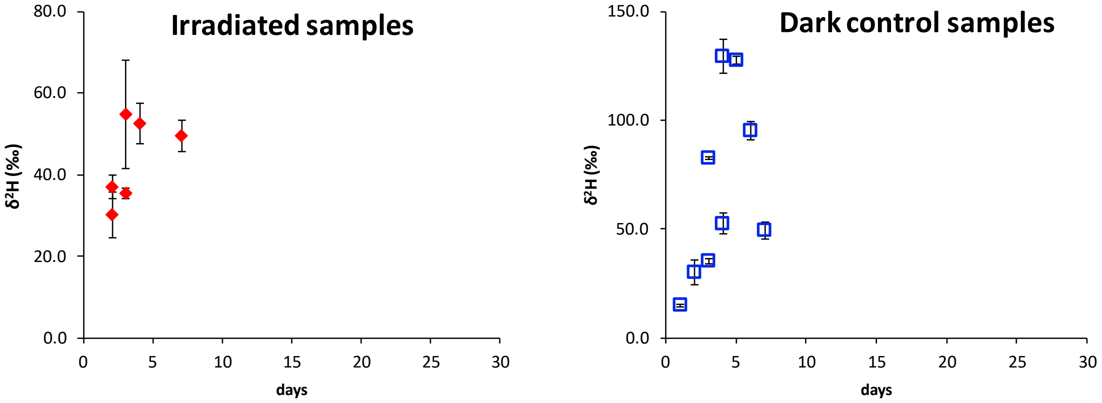

Figure 6. Hydrogen isotope composition of benzo(*a*)pyrene along the experiment in a) Arenosol soil and b) Regosol soil (below). Error bars represent the standard deviation between analytical duplicates.

Table 1. Photodegradation rates (%) of 16 PAHs under study in Arenosol and fine-textured Regosol soil when simulating the current Mediterranean climate and an IPCC-based climate change scenario

	Arenosol		**Fine-textured Regosol**	
	Current climate*	**Climate change****	**Current climate***	**Climate change****
Naphthalene	0	0	0	0
Acenaphthylene	0	0	0	0
Acenaphthene	1.5	21.3 [a]	2	2.6
Fluorene	2.9	15.4 [c]	9.5	7.8
Phenanthrene	11.2	16.0	33.2	30.5
Anthracene	19.7	85.4 [b]	39.8	36.4 [d]
Fluoranthene	0	28.9	12.5	14.1
Pyrene	0	60.1	17.1	18.6
Benzo(*a*)anthracene + chrysene	0	41.0	30	34.2
Benzo(*b*+*k*)fluoranthene	0	20.2	30	16.8
Benzo(*a*)pyrene	23.0	54.6	4.9 [c]	37.8 [d]
Benzo(*ghi*)perylene	3.6	27.1	24.6	19.5
Dibenzo(*ah*)anthracene	2.0	37.0	28.3	23.2
Indeno(*123-cd*)pyrene	11.7	39.1	68.9	43.2

*T= 20ºC; light intensity= 9.6W/m^2

** T= 24ºC; light intensity= 24W/m^2

Complete degradation after: [a]1 day, [b]4 days, [c]7 days, and [d]14 days.

Table 2. Information about metabolites identified in irradiated and dark controls in Arenosol and Fine-textured Regosol soils when simulating current climate scenario climate change scenarios.

Suggested name	m/z	T_R (min)	Arenosol soil				Regosol soil			
			Current climate		Climate change		Current climate		Climate change	
			RAD	DC	RAD	DC	RAD	DC	RAD	DC
Benzophenone	182	12.40	x	x	x	x	x	x	x	x
9H-fluorene,9-methylene	252	6.72	x	x			x	x		
Methyl dehydroabietate	299	14.45	x	x			x	x		
1,2-dihydrobenzo(*b*)fluoranthene	253	16.86	x	x			x	x	x	x
2,3-dihydrofluoranthene	202	12.22	x	x			x	x		
Acetophenone	120	6.93			x	x			x	x
Benzaldehyde,3-hydroxy-4-methoxy	151	9.85			x	x			x	x
Benzeneacetic acid	136	8.22			x	x			x	x
2,6-dimethylbenzaldehyde	133	7.95							x	x
9,10-anthracenedione	208	16.85	x	x	x	x	x	x	x	x
7H-benzanthrene / 11H-benzo(*b*)fluorene	281	20.32							x	x
Benzo(*a*)anthracene-7,12-dione	258	24.98	x		x		x		x	
1-acenaphthenol	168	12.91							x	
2-naphthalenecarboxaldehyde	184	16.20							x	
Naphthalic anhydride	198	17.74			x				x	
9H-fluoren-9-one	180	13.88			x					
1(2H)-acenaphthylenone	168	12.93			x					

RAD= irradiated sample; DC= dark control